Research Article

Long Wang, Xingyuan Huang*, and Duyang Wang

Solubility and diffusion coefficient of supercritical CO_2 in polystyrene dynamic melt

https://doi.org/10.1515/epoly-2020-0062
received July 27, 2020; accepted September 15, 2020

Abstract: The solubility and diffusion coefficient of supercritical CO_2 in polystyrene (PS) dynamic melt were studied by using a new constant pressure experimental device. By comparing the experimental results with those of other researchers, the validity of the experimental device and the reliability of the calculated results are verified. The solubility and diffusion coefficient of supercritical CO_2 in polystyrene dynamic melts at different temperatures and pressures were obtained. The numerical calculation method, dissolution process, and experimental results are analyzed and compared with that of the static melt. Finally, the effects of stirring speed, pressure, and temperature fluctuation on the solubility and diffusion coefficient are also analyzed.

Keywords: CO_2, PS, stirring, solubility, diffusion coefficient

1 Introduction

In recent years, with the development of polymer foam and porous material theory and technology, polymer composites have been widely used in interior panels in aircraft and boats (1), gas separation material (2,3), temperature and pressure sensors (4,5), catalyst supports (6,7), lightweight devices for electromagnetic interference shielding (8), and encapsulation agents for drug release (9,10). In the preparation of polymer foams and porous materials, supercritical CO_2 is widely used due to its excellent solubility, low cost, environmental protection, and other properties. A major advantage of supercritical CO_2 applications to polymers is that the morphology and processing conditions of polymers are greatly improved by the dissolved CO_2. The thermal properties and rheological properties of molten polymers are also changed, for example, the surface tension (11,12), viscosity (13,14), and the glass transition temperature (15,16) of the molten polymer decrease with the dissolution of CO_2.

We know that the key parameters of carbon dioxide in polymer applications are solubility and diffusion coefficient. Unlike the mature measurement system of thermal conductivity or viscosity, the measurement of mass transfer characteristics is often difficult due to the measurement of concentration and other complex problems during mass transfer. Several researchers have investigated the solubility and diffusivity of carbon dioxide in thermally softened or molten polymer systems. Sato et al. (17–20) have measured the solubility and diffusion coefficients of CO_2 in polymers across wide ranges of pressure and temperature. Aionicesei et al. (21) studied the solubility of nitrogen (N_2) and CO_2 into several polymers such as low-density polyethylene (LDPE), polypropylene (PP), polystyrene (PS), and high-density polyethylene (HDPE). Aionicesel et al. (22) studied the solubility of several gases including CO_2 in polyethylene (PE). Molecular simulations are also used to obtain solubility and diffusion coefficient of CO_2 in polymers (23,24). During the experimental measurement, researchers developed several experimental methods for measuring these parameters, such as the pressure decaying method (17), electro balance method (25,26), new type gravimetric method (27,28), and magnetic suspension balance method (29). However, due to the high cost of experimental instruments or the complicated and time-consuming experimental process, these experimental methods have not been widely used. Among them, the pressure decaying method is the most widely used because of its simplicity in experimental measurement.

When using the experimental data to establish a mathematical model to solve the diffusion coefficient,

* **Corresponding author: Xingyuan Huang,** Jiangxi Key Laboratory of High-Performance Precision Molding, Nanchang University, Nanchang 330031, China; Jiangxi Key Laboratory of Polymer Micro-Nano Manufacturing and Devices, East China, University of Technology, Nanchang 330013, China,
e-mail: huangxingyuan001@126.com
Long Wang: Jiangxi Key Laboratory of High-Performance Precision Molding, Nanchang University, Nanchang 330031, China; Institute of Technology. East China Jiao Tong University, Nanchang 330100, China
Duyang Wang: Jiangxi Key Laboratory of High-Performance Precision Molding, Nanchang University, Nanchang 330031, China

Open Access. © 2020 Long Wang *et al.*, published by De Gruyter. This work is licensed under the Creative Commons Attribution 4.0 International License.

the modeling of the physics interface usually requires complex mathematical solutions. The researchers obtained different mathematical solutions by modeling the boundary conditions of the gas–liquid interface with different methods (30–32). Due to the complexity of the gas–liquid interface, most researchers assume that the interface concentration is constant, thus simplifying the analysis method. However, this leads to a large error in the value of the diffusion coefficient. In addition, the research on solubility and diffusion coefficient is mainly focused on the static molten polymer, while the research on the dynamic molten polymer is less. In this paper, the solubility and diffusion coefficient of supercritical CO_2 in stirring PS are carried out by means of pin agitator.

2 Materials and methods

To obtain stable boundary conditions at the gas–liquid interface, our experimental team has finally designed a constant-pressure experimental instrument. The details of the experimental instrument are shown in Figure 1. The diffusion cell is made of stainless steel, cylindrical with an inner diameter of 12 cm, and has two holes: one for the gas intake from the gas storage cell and the other for vacuum extraction. It has a stainless steel cover on top and a hole for the thermocouple of the temperature sensor, which has an accuracy of ±0.1°C. The gas storage cell is also cylindrical with an inner diameter of 10 cm, made of stainless steel, and has three holes: one for the gas to enter the diffusion cell, another one is used to draw gas from the gas cylinder before diffusion begins, and the last one is also used to extract gas from the gas cylinder to keep the pressure constant after the diffusion started. In the process of diffusion, the piston in the gas storage cell is regulated by the gas above the piston to keep the pressure constant. The displacement information is sent to the computer through the displacement meter with an accuracy of ±0.05 mm and a signal acquisition frequency is 1 time/second. These two cells are kept in the oil pool that can be heated up to 300°C.

In preparing for the experiment, first of all, we should make sure that the system is leak-free. Pressurize the device and place it for about one day to determine if the system has any leaks. Using the high resolution of the pressure sensor, which has an accuracy of ±0.01 MPa, any minor leakage can be detected from the experimental unit. If a leak is found, a leak detector can be used to determine the leak location. For constant pressure test, gas leakage is a very serious problem. After the completion of the gas tightness test, each experiment can be carried out according to the following steps:

1. First, a certain number of polymer samples are weighed on a scale and placed into the diffusing cells. Then, lock

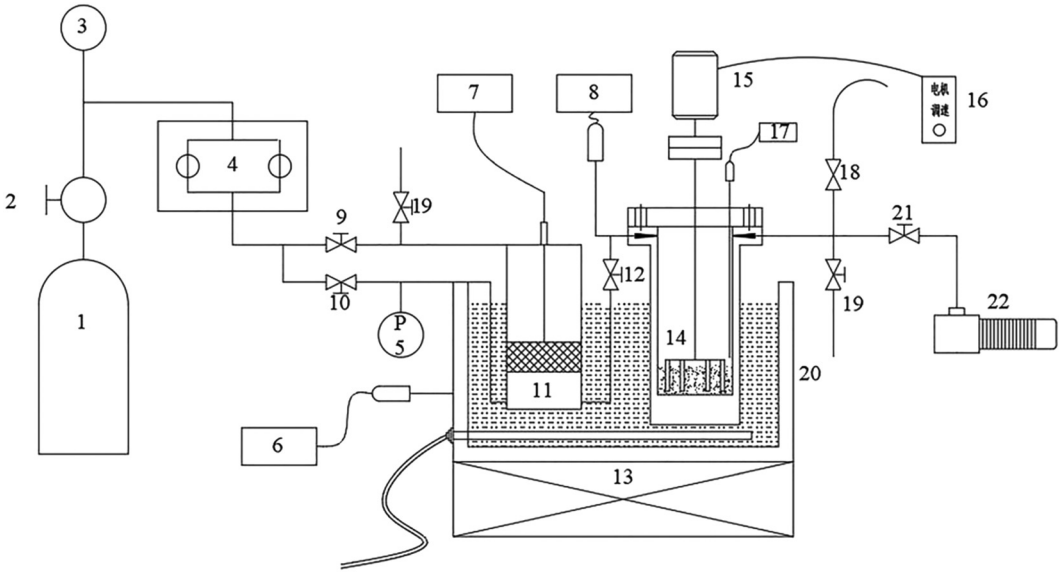

Figure 1: Schematic diagram of experimental apparatus for constant pressure method. 1 – gas cylinder, 2 – gas pressure reducer, 3 – pressure gage, 4 – booster pump, 5 – electric contact pressure gauge, 6 – temperature controller, 7 – displacement meter, 8 – pressure instrument, 9 – pressure retaining valve, 10 – intake valve, 11 – gas storage cell, 12 – inflow valve, 13 – lifting platform, 14 – diffusion cell, 15 – stirring element, 16 – stirring speed controller, 17 – temperature sensor, 18 – safety valve, 19 – vent valve, 20 – oil bath, 21 – vacuum valve, and 22 – vacuum pump.

the lid, open valve 12, close 9 and 10, and vacuum the gas storage cell and diffusion cell, so that the piston in the gas storage cell reaches the bottom.
2. Open valve 10, close valve 9 and 12, and introduce gas from the gas cylinder into the gas storage cell through the plunger pump, so that the piston is rising until the pressure of the gas storage cell reaches the specified value (up to 35 MPa).
3. After two cells are heated to the specified temperature through the oil pool, open valve 9 and 12, and close valve 10. Then, gas flows from the storage cell to the diffusion cell, and it is also introduced simultaneously to the upper of the storage cell's piston from the gas cylinder to maintain the specified pressure value.
4. After the diffusion starts, according to the pressure gauge information the gas is automatically introduced into the upper of the storage cell's piston to keep the pressure constant. At the same time, the displacement information is transferred to the computer through the displacement sensor until the diffusive equilibrium.

To verify the reliability and reasonable of our experimental device and mathematical model under the constant-pressure method, we first selected four groups of experiments under different experimental conditions to measure the solubility and diffusion coefficient of CO_2 + PS. Experimental conditions were selected from the work of other researchers (19), who obtained the solubility and diffusion coefficient under the same experimental conditions. We compared the values of ours with the reported values of theirs. All the comparative data came from public data from the researchers. Experimental conditions are summarized in Table 1.

To carry out the experiment under dynamic conditions, the stirring element of the pin was designed to model the pin screw commonly used in the continuous extrusion of microporous plastics. The pin is made of stainless steel, cylindrical with a diameter of 4 mm, and the height can be adjusted according to the experimental requirements. As shown in Figure 2, by changing the stirring element, we can conduct experiments in both static and dynamic conditions. To compare the solubility and diffusion coefficient of CO_2 + PS under static and dynamic conditions, three groups of experiments were selected. The experimental conditions are listed in Table 2, and the stirring speed is 2 (rpm).

The materials used in the experiment are as follows: CO_2 (>99.5% purity) was obtained from Guohui Gas Co. Ltd (Nanchang, China). All chemicals were used as received. Polystyrene (PS, >99.7% purity, T_g = 381.4 K, M_n = 10^5) was supplied by Taihua polystyrene Co. Ltd (Ningbo, China). All the characteristics of polystyrene were given by the supplier.

3 Theories and mathematical model

The mass transfer of a substance can be divided into molecular mass transfer or convection processes as a result of fluid motion. Molecular mass transfer, also known as molecular diffusion, is a phenomenon of material transfer caused by the irregular thermal movement of molecules. Molecular diffusion can occur in gas, liquid, and solid phases. Convection diffusion is the mass transfer process caused by the macroscopic movement of fluid, usually refers to the mass transfer process between the moving fluid and the solid surface, or between two finitely miscible moving fluids. In this experiment, considering that no chemical reaction occurs in the CO_2 + PS system, as shown in Figure 3, it can be seen that the mass transfer under the static condition is molecular diffusion. Under dynamic conditions of pin stirring in our experiments, there is no longitudinal or radial flow due to the type of stirring element used in the diffusion cell, and the CO_2 concentration in angular direction is uniform. We believe that the main mode of material transfer is still molecular diffusion. In these experiments, although the material transfer mode under both static and dynamic conditions is molecular diffusion, the shear action due to the stirring element produces a velocity gradient in the polymer melt that resulting in the relative motion of the polymer melt

Table 1: Summary of experiments conducted under the same experimental conditions with other researchers

Experiment no.	Temperature (K)	Pressure (MPa)	Dissolve system	The diffusion condition	Liquid height H (cm)
1	423	2.5	CO_2 + PS	Static	1.0 and 2.0
2		4.5			
3	473	2.5			
4		4.5			

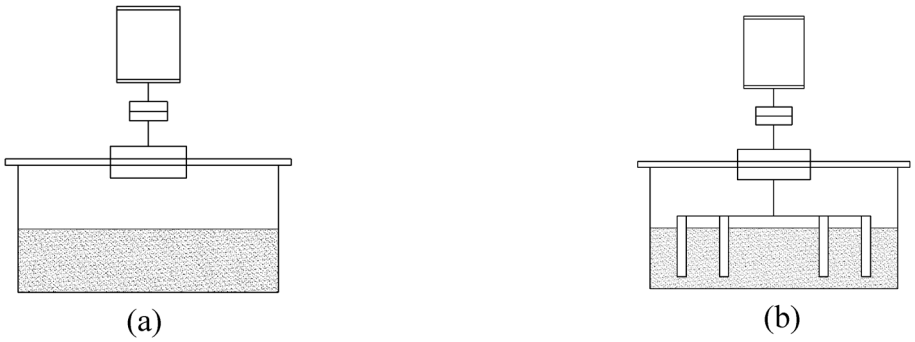

Figure 2: The diffusion cell under static or dynamic conditions. (a) No stirring (static condition). (b) Pin stirring (dynamic condition).

Table 2: Summary of experiments conducted under static and dynamic conditions (2 rpm)

Experiment no.	The temperature (K)	The pressure (MPa)	Dissolve system	The diffusion condition	Liquid height H (cm)
4	443	7.5, 8.5, 9.5	CO_2 + PS	Static & dynamic	1.0
5	453	7.5, 8.5, 9.5			
6	463	7.5, 8.5, 9.5			

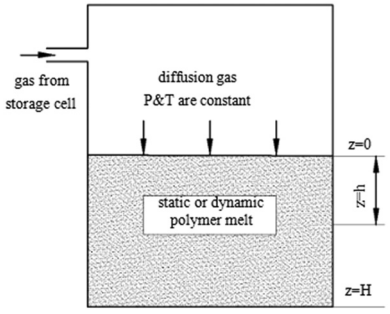

Figure 3: Schematic graph of the diffusion model.

and the direction of the polymer chain oriented. The larger the velocity gradient is, the greater the orientation will be, and the previously irregular molecular chains will become orderly, thus homogenizing the intermolecular holes and increasing the number of holes. In addition, the ordered arrangement of polymer chains shortens the distance of gas molecules dissolving and reduces the distance of gas concentration gradient diffusing in the polymer melt. Finally, the time to reach equilibrium concentration is shortened.

In molecular mass transfer, if we ignore the interfacial resistance, there are two key parameters in gas dissolved in liquids. The first is solubility, which is the maximum concentration of gas dissolved in liquid. Thermodynamically, since the pressure and temperature in the diffusion unit are constant, namely, no pressure gradient, so it is reasonable to assume an instantaneous equilibrium at the gas–liquid interface. As Sheikha et al. (33) have explained, the equilibrium concentration at the gas–liquid interface is the maximum concentration of dissolved gas (i.e., solubility) in the liquid. To our constant pressure experiment device, due to the constant pressure and temperature in the diffusion cell, gas can get the stable solubility at the gas–liquid interface during the experiment. The second is the diffusion coefficient, which determines how quickly the gas dissolves in the liquid and can be obtained from the experimental data. As shown in Figure 3, the gas diffuses to the liquid along with a cylinder with a length of H, one end of the liquid and the cylinder surface are sealed, while the other end keeps the gas at stable in maximum dissolution concentration. Considering that the diffusion process is a one-dimensional unsteady process, Fick's second law can be used to solve it:

$$\frac{\partial C_g}{\partial t} = D\frac{\partial^2 C_g}{\partial z^2}, \tag{1}$$

where C_g is the concentration of the gas in the liquid at distance Z and time t; Z is the distance from the gas–liquid interface; t is the time; and D is the diffusion coefficient (in square meters per second). In using the above formula, we used the following assumptions to determine the diffusion coefficient. First, there is a very thin contact surface between the gas and the liquid, which is in an equilibrium state, and the dissolved gas in the liquid is in a saturated state at the contact surface. Second, the temperature and pressure in the diffusion cell are constant. Third, the diffusion coefficient was treated as a constant. Fourth, the thickness of the polymer H was assumed to be constant during the diffusion. Since our experimental

device is a constant temperature and pressure device and the amount of dissolved gas in our experiment is small, these assumptions can be considered reasonable.

Some initial and boundary conditions are required to solve Eq. 1. When dissolution has not begun:

$$C_g(z, t = 0) = 0 \quad (H \geq z \geq 0) \tag{2}$$

As mentioned above, for our experimental device, since the pressure and temperature in the diffusion cell are constant, the stable equilibrium concentration at the gas–liquid interface is the maximum concentration of the gas in the liquid, which is one of the main advantages of our constant pressure apparatus, so the following boundary condition is obtained:

$$C_g(z = 0, t) = C_g^* \quad (t > 0), \tag{3}$$

where C_g^* is the maximum concentration or solubility of the gas in the liquid. Indeed, it is easier to solve Eq. 1 with constant boundary conditions than with the time-dependent boundary conditions used by other researchers (30).

For the second boundary condition in the finite field, we can consider that the rate of change of concentration at the bottom of the diffusion chamber is zero. Therefore, the second boundary condition can be written as follows:

$$\frac{\partial C_g}{\partial z}(z = H, t) = 0 \quad (t > 0) \tag{4}$$

Next, we use these boundary conditions to get the mathematical solutions. As we know, the diffusion coefficient of CO_2 in the dissolution process of the polymer can be regarded as a function of the concentration of CO_2, which keeps falling as the concentration of CO_2 increases. In this experiment, the concentration change of CO_2 in the experimental sample can be calculated by the amount of CO_2 dissolved, and the calculation formula is as follows:

$$m(t) = \frac{PV_g(t)M}{ZTR}, \tag{5}$$

where $m(t)$ is the amount of gas mass change in the gas storage cell at time t; $V_g(t)$ is the volume change of the gas storage cell at time t; and P, T, R, Z, and M represent pressure, test temperature (K), universal gas constant, gas compressibility factor, and molar mass, respectively, where the compression factor Z can be obtained by the literature (34).

In our experiment, pressure and temperature are constant, we can consider that the concentration of CO_2 at the gas–liquid interface is a stable equilibrium concentration. The amount of gas mass change in gas storage cell at time t is equal to the amount of gas dissolved into the liquid, and the rate of gas mass change in gas storage cell is equal to the rate of the gas diffusing into the polymer at the gas–liquid interface. Therefore, we can now measure the dissolution rate of the gas using the Fick's first law:

$$\frac{dm(t)}{dt} = -DA\left(\frac{\partial Cg}{\partial z}\right)_{z=0}, \tag{6}$$

where A stands for the cross-sectional area of the diffusion cell. Then, integrate both sides of Eq. 6 from 0 to t and get Eq. 7:

$$m(t) = \int_{t=0}^{t} \frac{dm(t)}{dt} dt = \int_{t=0}^{t} -DA\left(\frac{\partial Cg}{\partial z}\right)_{z=0} dt. \tag{7}$$

To solve the diffusion coefficient (D) in Eq. 7, we first need to find the concentration function (C_g). The analytical solution of the problem under the boundary conditions of finite field Eq. 4 are obtained by Laplace transform method as follows (35):

$$C_g(z, t) = C_g^*\left[1 - \frac{4}{\pi}\sum_{n=1}^{\infty}\frac{1}{2n-1}\exp\left(-\frac{D(2n-1)^2\pi^2 t}{4H^2}\right)\sin\frac{(2n-1)z\pi}{2H}\right]. \tag{8}$$

By substituting Eq. 8 into Eq. 7, the following equation can be obtained:

$$m(t) = \frac{8AC_g^*H}{\pi^2}\sum_{n=1}^{\infty}\frac{1}{(2n-1)^2}\left[1 - \exp\left(-\frac{D(2n-1)^2\pi^2 t}{4H^2}\right)\right]. \tag{9}$$

Finally, Eq. 5 and 9 are solved simultaneously to obtain the following equation:

$$\frac{PV_g(t)M}{ZTR} = \frac{8AC_g^*H}{\pi^2}\sum_{n=1}^{\infty}\frac{1}{(2n-1)^2}\left[1 - \exp\left(-\frac{D(2n-1)^2\pi^2 t}{4H^2}\right)\right]. \tag{10}$$

The above equation relates our experimental measurements to the prediction of diffusion coefficient D and solubility C_g^*. Using the volume change of the gas storage cell at time $t(V_g(t))$, the two unknowns can be determined by the graphical method. Next, we take an example to illustrate the graphical method in detail.

3.1 Solution of D and C_g^*

We know that the infinite series on the right-hand side of Eq. 10 converges quickly and is approximately

equal to its first term, so Eq. 10 can be written as follows:

$$m(t) = \frac{8AC_g^* H}{\pi^2}\left[1 - \exp\left(-\frac{D\pi^2 t}{4H^2}\right)\right]. \quad (11)$$

Here, first we take the derivative of both sides with respect to time t, and then we take the log of both sides, finally, we get the following expression:

$$\ln\left(\frac{dm(t)}{dt}\right) = \ln\left(\frac{2AC_g^* D}{H}\right) - \frac{D\pi^2}{4H^2}t. \quad (12)$$

Equation 12 can be regarded as a linear function of $\ln(dm(t)/dt)$ over time t, and the diffusion coefficient D and solubility C_g^* can be obtained through the slope and intercept of the equation. However, not all data from the experiments is linear with time t and only data that satisfy the linear relationship are most useful, which is illustrated by Figure 4. In addition, it should be noted that due to the fluctuation of experimental data, we need to smooth the experimental data first and then find the derivative of $m(t)$ with respect to t.

As can be seen from the distribution of experimental data in Figure 4, the dissolution process is divided into three stages. The first stage is the rapid dissolution stage, and the dissolution rate is fast and stable. We think at this stage, the gas has not spread to the bottom of the diffusing cell, but this stage does not last long and the amount of gas dissolved is little. The second stage is the stable diffusion stage, the dissolution rate decreases steadily, $\ln(dm(t)/dt)$ and time t meet the linear relationship, the time is relatively long, about 80% amount of solubility is completed in this stage. The third stage belongs to the late stage of diffusion, and the diffusion is nearly completed. At this stage, due to the small amount of dissolution, the control requirements on experimental instruments are high, and the experimental data fluctuate greatly.

Surely, for the graphical method, only the data from the second stage, even a portion of the data of the second stage is needed to calculate the diffusion coefficient and solubility.

4 Results and discussion

4.1 Validation of results

The experiments listed in Table 1 are to verify our experimental device and calculation method. Through the graphical method, the linear parts and comparison data of the four groups of experiments (liquid height: 1 cm) are shown in Figure 5 and Table 3. As can be seen from Table 3, our solubility is similar to that of Sato et al., but our diffusion coefficient is much higher. However, there is no reliable way to prove that results are more reliable. Here, we only compare the increments or ratios of values calculated at different temperatures or pressures. The solubility difference and the diffusion coefficient ratio between different experiments are also reported in Table 3. As shown in Table 3, the diffusion coefficient and solubility obtained of ours have similar consistency with those of Sato et al.

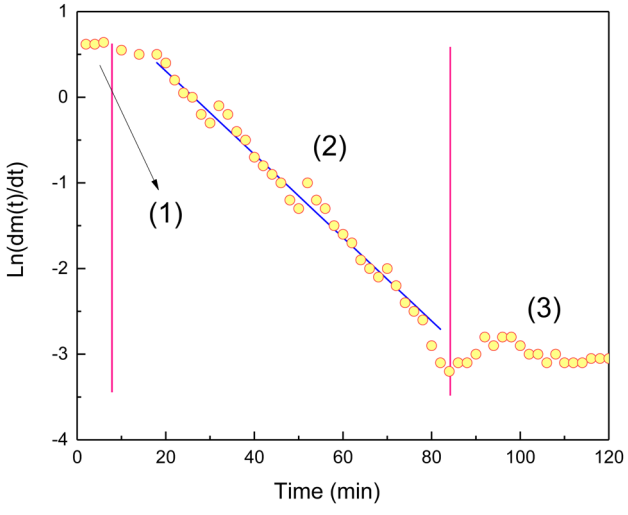

Figure 4: Schematic graph of the dissolving process.

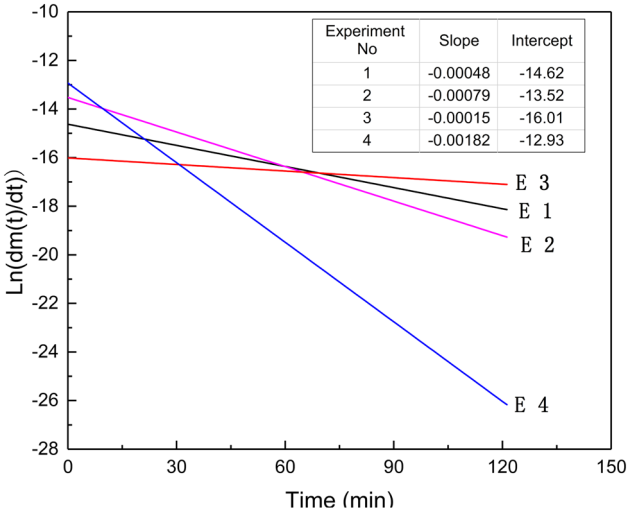

Figure 5: Linear fitting of the second stage of the experiments in Table 1 (liquid height: 1 cm).

Table 3: Comparison of solubility and diffusion coefficient with the results of other researchers

Exp. no.	P (MPa)	T (K)	Our work		Sato et al.'s work	
			Solubility (g-CO_2/g-PS)	Diffusion coefficient (10×10^{-8} m^2/s)	Solubility (g-CO_2/g-PS)	Diffusion coefficient (10×10^{-10} m^2/s)
1	423	2.5	0.01005	1.96	0.01017	3.01
2		4.5	0.01858	3.19	0.01845	4.72
3	473	2.5	0.00814	6.05	0.00831	9.24
4		4.5	0.001451	7.38	0.01482	10.5
The solubility difference		Experiments 1 and 2		0.00853	0.00828	
		Experiments 3 and 4		0.00637	0.00651	
The diffusion coefficient ratio		Experiment 2/experiment 1		1.63	1.57	
		Experiment 4/experiment 3		1.22	1.14	

To further verify our experimental device and calculation method, using the solubility and diffusion coefficient obtained from the experiments (liquid height: 1 cm) in Table 1, we obtained the analytical solution of Eq. 11. Then, the experiments (liquid height: 2 cm) were conducted, and the comparison of experimental data with the analytical solution is shown in Figure 6. As can be seen from Figure 6, the analytical solution and the experimental data are consistent in the whole dissolution process. It also can be seen from the comparison graphs that when the concentration of CO_2 in PS is small, the analytical solution and the experimental data are more consistent. However, when the concentration of CO_2 in PS increases gradually, the trend of data fluctuation in the later stage will increase.

It is only true that our constant pressure device ensures the constant pressure of the diffusion cell by adjusting the amount of gas injection, which has a certain "lag". If the experimental pressure is higher or the gas dissolution rate is fast, it is difficult to ensure the accurate injection amount, and there is an error between the measured pressure value and the actual value. In the later stage of the experiment, the fluctuation of this error will increase due to the decrease of the dissolved amount of gas. Although the pressure fluctuates greatly in the later stage of the experiment, it is stable in the early stage, and such fluctuation will not affect the predicted value obtained with our graphical methods.

4.2 Comparison of static and dynamic conditions

The experiments listed in Table 2 are to compare the solubility and diffusion coefficients under static and dynamic conditions at different temperatures and pressures. Using the graphical method, the linear parts of the experiments (P = 7.5 MPa) under static and dynamic conditions are presented in Figure 7. The time of the linear stages of all experiments is also reported in Table 4. The calculation results of solubility and diffusion coefficient of experiments are listed in Table 5.

It can be seen from Figure 7 that the linear parts of the experiments under static and dynamic conditions have an intersection point, we call this point the velocity intersection point. The time of velocity intersection point is also listed in Table 4. In the initial stage of dissolution, stirring makes the dissolution rate of CO_2 much higher than that under static conditions. But as the amount of CO_2 in the polymer increases, the diffusion resistance of CO_2 increases rapidly under dynamic conditions, and stirring also accelerate the escape of CO_2 molecules. After crossing the time of the velocity intersection point, the amount of CO_2 dissolved under dynamic condition gradually enters a stable and slow growth stage, and the dissolution rate is even lower than that under static conditions.

Before we compare the solubility and diffusion coefficients under dynamic conditions, we first need to verify the reliability of the results under dynamic conditions. Since most researchers mainly study these parameters under static conditions, we cannot compare with other research results, but we can verify our results through experiments. Three experiments (liquid height = 2 cm) under dynamic conditions were conducted, and the comparison of experimental data with an analytical solution obtained from the experiments (liquid height = 1 cm) is shown in Figure 8. It is only true that the analytical solution and the experimental data are consistent.

As can be seen from Table 5, the trends of all the values of the diffusion coefficient and solubility are reasonable, the diffusion coefficient increases with temperature while the

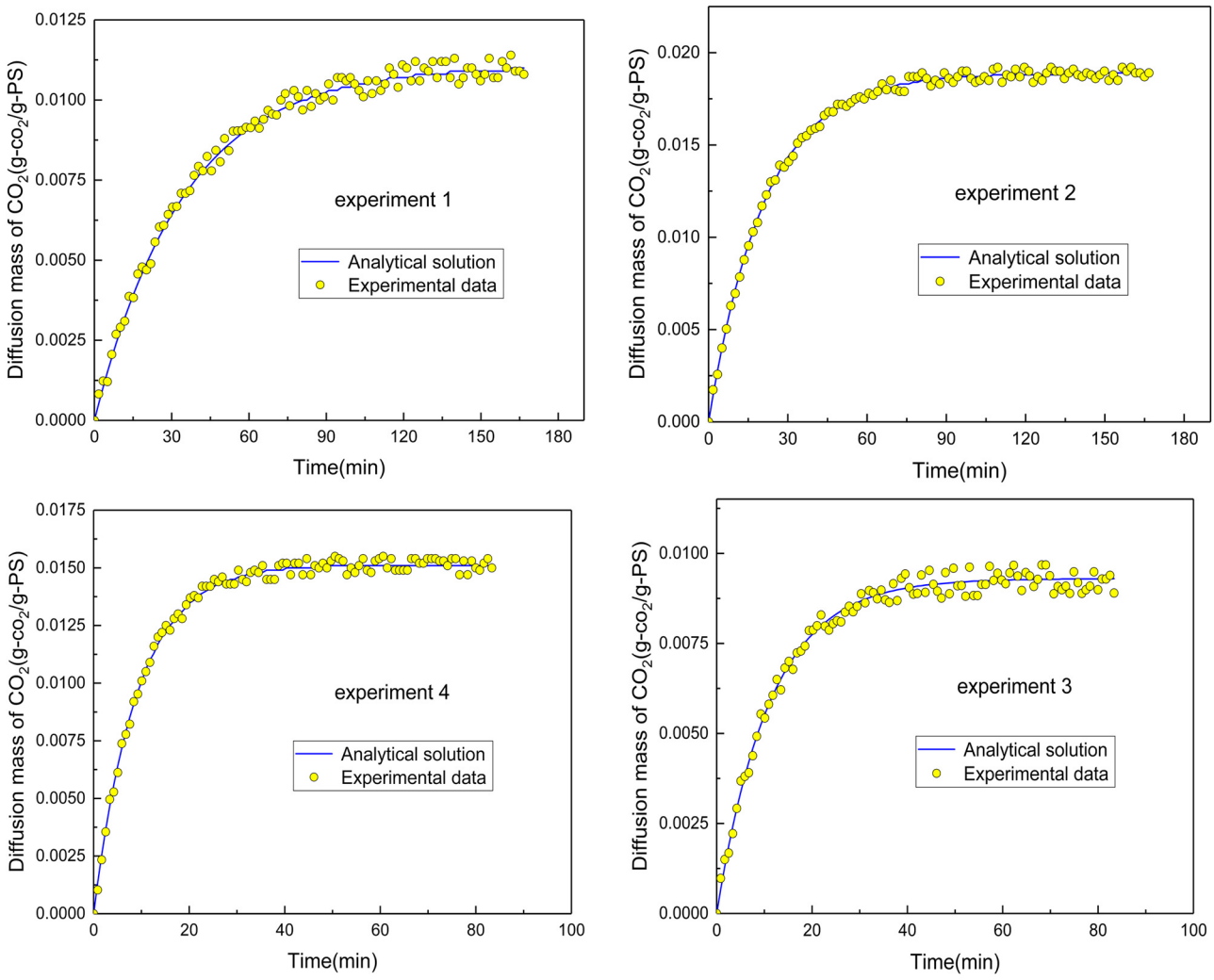

Figure 6: Comparison of the experimental data (liquid height: 2 cm) with the analytical solution under static conditions.

solubility decreases, diffusion coefficient and solubility both increase with increasing pressure. At the same temperature and pressure, the dynamic diffusion coefficient is much higher than the static diffusion coefficient, and the solubility is similar. The main factors affecting solubility are still temperature and pressure. This is due to stirring that not only makes CO_2 molecules in full contact with the polymer but also makes the irregular polymer molecular chain orderly, shortening the dissolution distance of gas molecules, reducing the concentration gradient distance of gas diffusion in the polymer melt, and shortening the time to form a uniform system. Ultimately, stirring reduces the time to equilibrium. However, as can be seen from Table 4, the difference in equilibrium time between static and dynamic conditions is much smaller than that between diffusion coefficients. This is because in the later stage of diffusion, as the concentration of CO_2 in the liquid increases, agitation also accelerates the escape of CO_2 molecules and the fluctuation of concentration, thus increasing the equilibrium time.

It is also noted that the solubility under static and dynamic conditions is not much different, but the solubility under dynamic conditions is sometimes slightly higher than that under static conditions. This is because the stirring homogenizes the pores between the molecules, increases the number of pores, and makes the local gas molecules more closely arranged, but stirring also accelerates the escape of carbon dioxide molecules. In general, stirring does not make a significant change in solubility. Finally, the dissolution curves of all experiments under dynamic conditions in Table 2 are plotted in Figure 9.

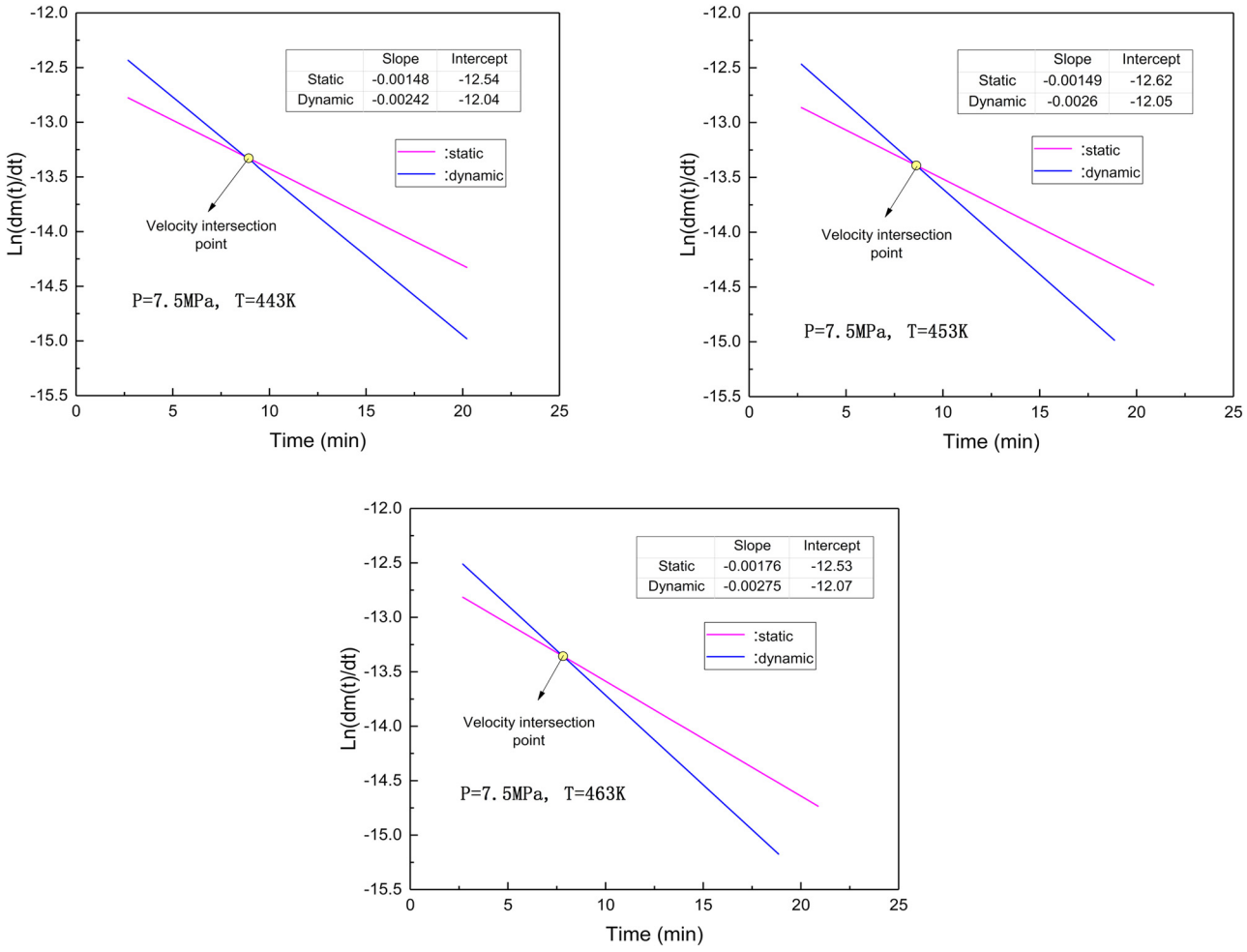

Figure 7: Linear fitting of the second stage (P = 7.5 MPa, T = 443–463 K) under static and dynamic conditions.

4.3 The effect of stirring speed.

To further study the effect of the stirring speed on the dissolution rate, experiments with different stirring speeds were carried out under the experimental conditions of P = 7.5 and T = 433 K. The solubility and diffusion coefficients are shown in Table 6, and the dissolution curves are plotted in Figure 10.

It can be seen from Figure 10 that the change of mixing speed has little influence on the solubility, but it has a great influence on the dissolution rate or diffusion coefficient. Due to the entanglement between the

Table 4: The time of the linear stages of the experiments in Table 2 (static/dynamic)

P (MPa)	T (K)	The time of end linear behavior (min)	The percentage of solubility at the beginning of scattering (%)	The time of end diffusion process (min)	The time of velocity intersection point (min)
7.5	443	20/15	74/80	45/35	9
	453	20/14	76/80	40/33	8.5
	463	21/15	86/81	34/27	8
8.5	443	18/14	78/82	46/39	7.5
	453	16/12	82/80	43/37	6.5
	463	16/13	79/83	42/36	6
9.5	443	24/16	85/88	51/44	6
	453	15/13	84/87%	50/41	5.5
	463	15/13	86/85	48/40	5

Table 5: The solubility and diffusion coefficient of the experiments in Table 2

P (MPa)	*T* (K)	Static condition		Dynamic condition (2 rpm)	
		Solubility (g-CO_2/g-PS)	Diffusion coefficient (10 × 10^{-8} m^2/s)	Solubility (g-CO_2/g-PS)	Diffusion coefficient (10 × 10^{-8} m^2/s)
7.5	443	0.0265	5.985	0.0268	9.826
	453	0.0242	6.025	0.0246	10.531
	463	0.0224	7.136	0.0228	11.142
8.5	443	0.0295	7.258	0.0298	11.647
	453	0.0269	8.165	0.0267	12.535
	463	0.0252	9.227	0.0254	13.651
9.5	443	0.0332	9.316	0.0331	13.512
	453	0.0295	10.221	0.0297	14.873
	463	0.0283	10.986	0.0282	15.428

molecular chain, the polymer viscosity is very high. Stirring can untangle the entanglement and reduce the flow resistance, viscosity, diffusion resistance between molecules, thus increasing the dissolution rate and diffusion coefficient of CO_2. With an increase in stirring speed and the number of untangled molecular chains, the diffusion coefficient continues to increase, while the viscosity continues to decrease. In other words, the diffusion

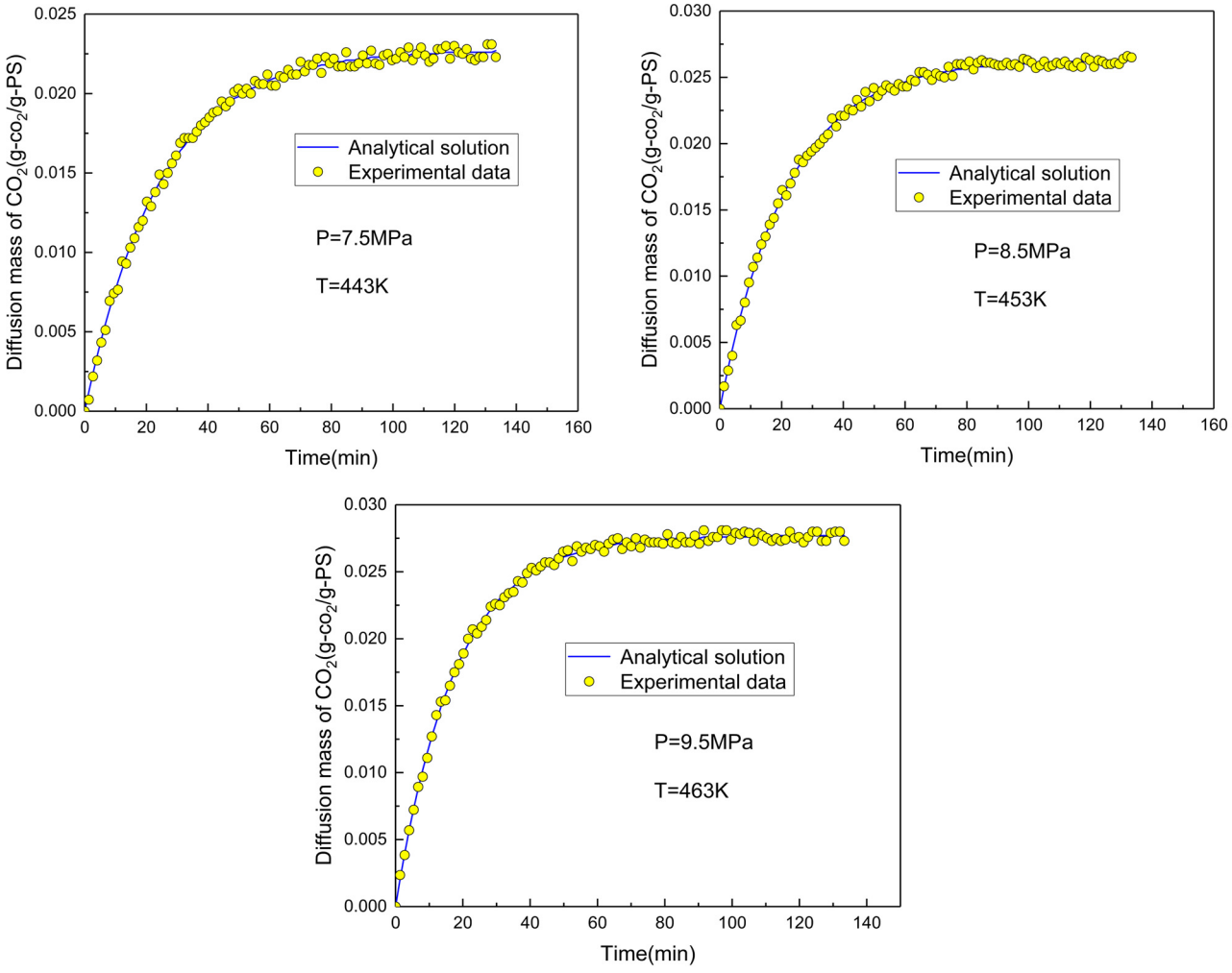

Figure 8: Comparison of the experimental data (liquid height: 2 cm) with the analytical solution under dynamic conditions.

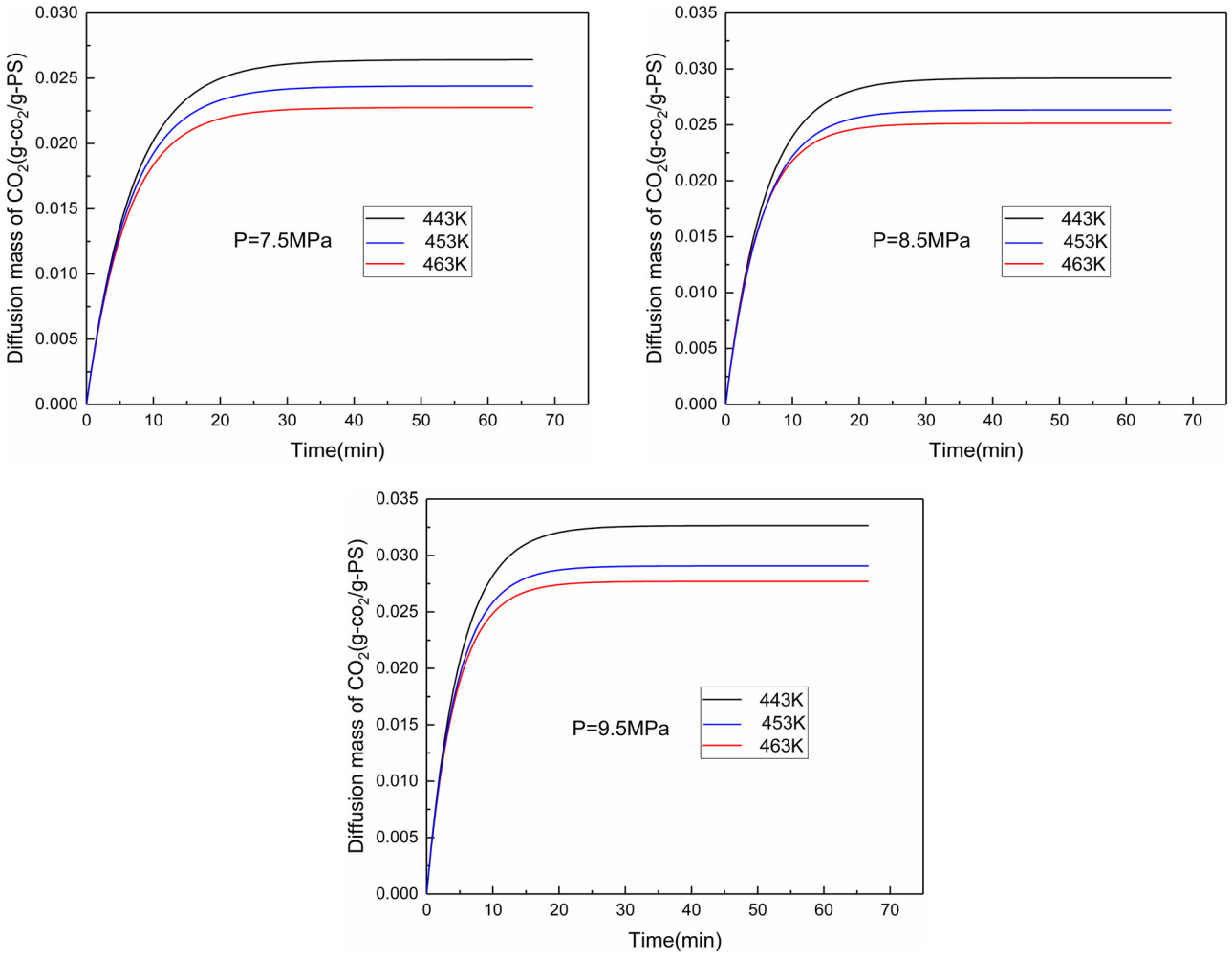

Figure 9: Dissolution curves under different temperatures and pressures at a mixing speed of 2 rpm.

Table 6: The solubility and diffusion coefficient under 0–4 cycles per minute at P = 7.5 MPa and T = 433 K

Stirring speed (rpm)	Solubility	Diffusion coefficient
0 (static)	26.5	5.985
2	26.8	9.826
3	26.3	11.513
4	26.6	12.375

coefficient increases as the viscosity decreases. We also note that since the number of molecular chains is finite, the number of newly untangled molecular chains should decrease with the stirring rate increasing. Therefore, the increasing degree of diffusion coefficient decreases with an increase in the stirring rate. As shown in Figure 10 and Table 6, the initial stirring speed (2 rpm) increased the diffusion coefficient significantly, but the degree of increase gradually decreased with an increase in the stirring speed.

4.4 Description of bar-climbing and the effect of pressure and temperature fluctuation

We know that for viscoelastic fluid, due to the difference in normal stress, the fluid is stretched along the stirring axis, and climbs the axis in the stirring process, which is called the bar-climbing phenomenon. If there was a bar-climbing effect in experiments with stirring, the path of gas diffusion into the polymer would be reduced, which could reduce the saturation time and increase the diffusion coefficient greatly. In our experiments, the stirring element of the pin always moves in a circle along with the molecular chain during the stirring process for the same rate and the liquid column is 1 cm, and the height of the pin agitator in the liquid is only 0.8 cm. It is so small that after the experiment, we detected the polymer trace on the surface of the pin agitator and found that the height of the polymer trace was not significantly

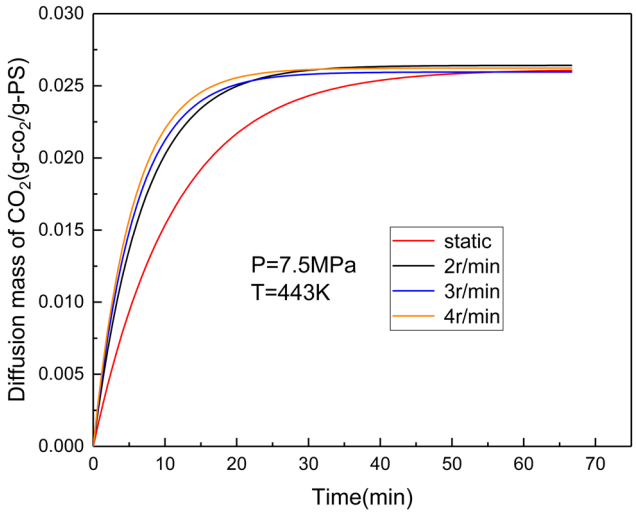

Figure 10: The diffusion mass of CO_2 versus time under different mixing rate at P = 7.5 MPa and T = 443 K.

different from the initial theoretical height. Thus, we do not think there is an obvious appearance of bar-climbing and can ignore the influence of bar-climbing in our experiments.

In our experiment, the constant pressure is maintained by the movement of the piston in the gas storage cell, and the piston movement is not continuous, but intermittent. Each time the piston moves downward, a transient high pressure is created within the diffusion cell. The temperature of the diffusion cell is heated by the oil. When the experiment time is longer or the weather is colder, the actual temperature of the diffusion cell also varies slightly due to heat conduction. Hence, the actual pressure and temperature of the diffusing cell may be slightly different than the target pressure and temperature.

In the above calculation, we did not consider these experimental errors; hence, there may be some errors in the calculation results. But this error can be corrected by using the following equation:

$$m_{act}(t) = m(t) - \Delta m_{fluc}(t) = \frac{PV_gM}{ZTR} - \left(\frac{P_{act}(t)}{T_{act}(t)} - \frac{P}{T}\right)\frac{V_gM}{ZR} = \frac{PV_gM}{ZTR} - \Delta P/T\frac{V_gM}{ZR}, \quad (13)$$

where $\Delta m_{fluc}(t)$ is the gas diffusion mass error due to pressure and temperature fluctuations. Now, $m(t)$ is corrected by the $\Delta m_{fluc}(t)$. $P_{act}(t)$ and $T_{act}(t)$ are the average actual pressure and temperature of the diffusion cell at period t, respectively, which can be calculated by recorded pressure and temperature during experiments. $\Delta_{P/T}$ is the average fluctuation values of pressure and temperature in diffusion cell, and the relative error $(1 - m_{act}(t)/m(t))$ of all experiments under dynamic conditions in Table 2 is also reported in Table 7.

As listed in Table 7. the corrected value is close to the uncorrected value with an error of less than 1%, indicating that the error caused by pressure and temperature fluctuation in the experiments is not significant.

5 Conclusions

According to the experimental data, the diffusion coefficient of CO_2 in polymer melts increases significantly even under low-speed stirring conditions, but the increasing degree of diffusion coefficient decreases with an increase in the stirring rate. Although stirring reduces the time for CO_2 to reach equilibrium in polymer melts, the difference is far less than that between diffusion coefficients,

Table 7: Average fluctuation of pressure and temperature and relative error % of all experiments (dynamic condition) in Table 2

P (MPa)	T (K)	Average fluctuation (kPa/K)	Relative error%	Without correction		With correction	
				Solubility (g-CO_2/g-PS)	Diffusion coefficient (10×10^{-8} m^2/s)	Solubility (g-CO_2/g-PS)	Diffusion coefficient (10×10^{-8} m^2/s)
7.5	443	−0.016	−0.09	0.0268	9.826	0.0268	9.826
	453	−0.015	0.087	0.0246	10.531	0.0246	10.531
	463	−0.057	0.35	0.0228	11.142	0.0229	11.145
8.5	443	0.066	0.34	0.0298	11.647	0.03	11.651
	453	−0.063	−0.33	0.0267	12.535	0.0266	12.528
	463	−0.018	−0.1	0.0254	13.651	0.0254	13.651
9.5	443	−0.026	−0.12	0.0331	13.512	0.033	13.511
	453	0.024	0.12	0.0297	14.873	0.0297	14.873
	463	−0.227	−0.11	0.0282	15.428	0.0281	15.426

because stirring also accelerates molecular escape and concentration fluctuations, thus increasing the equilibrium time. Low speed stirring may increase the solubility slightly, but the increasing degree is very small, which has little influence on the solubility as a whole. Based on the constant pressure experimental device and the graphic method, there will be some fluctuation of experimental data in the later stage, but we do not need to wait for the end of the experiment. As long as we can find some stable data for the linear part, we can draw the line and get the final result by slope and intercept.

Acknowledgments: Our team would like to express our sincere thanks to the National Science Foundation of China (grant nos. 51403615 and 51863014) for financial support. This work was also supported by the Special Fund Project of graduate student innovation in Jiangxi (grant no. YC2019-B022).

References

(1) Xia CL, James L, Tomy W, Christopher M. Polyurethane/clay nanocomposites foams: processing, structure and properties. Polymer. 2005;46(3):775–83.
(2) Wood CD, Tan B, Trewin A, Su F, Rosseinsky MJ, Bradshaw D, et al. Microporous organic polymers for methane storage. Adv Mater. 2010;20(10):1916–21.
(3) Lu X, Jin D, Wei S, Wang Z, An C, Guo W. Strategies to enhance CO_2 capture and separation based on engineering absorbent materials. J Mater Chem A. 2015;3(23):12118–32.
(4) Dan L, Elias AL. Flexible and stretchable temperature sensors fabricated using solution-processable conductive polymer composites. Adv Healthc Mater. 2020;9(16):2000380.
(5) Hu Y, Zhao T, Zhu P, Zhang Y, Liang X, Sung R, et al. A printable and flexible conductive polymer composite with sandwich structure for stretchable conductor and strain sensor applications. 2017 18th International Conference on Electronic Packaging Technology (ICEPT). IEEE, 2017.
(6) Zhang Y, Zhao L, Patra PK, Ying JY. Synthesis and catalytic applications of mesoporous polymer colloids in olefin hydrosilylation. Adv Synth Catal. 2010;350(5):662–6.
(7) Pierre SJ, Thies JC. Covalent enzyme immobilization onto photopolymerized highly porous monoliths. Adv Mater. 2010;18(14):1822–6.
(8) Singh AK, Shishkin A, Koppel T, Gupta N. A review of porous lightweight composite materials for electromagnetic interference shielding. Compos Part B Eng. 2018;149: 188–97.
(9) Santhosh KK, Bhooshan KV, Pradip P. Recent advancement in functional core-shell nanoparticles of polymers: synthesis, physical properties, and applications in medical biotechnology. J Nanopart. 2013;2013:1–24.
(10) Jackson EA, Hillmyer MA. Nanoporous membranes derived from block copolymers: from drug delivery to water filtration. ACS Nano. 2010;4(7):3548–53.
(11) Chiou JS, Barlow JW, Paul DR. Plasticization of glassy polymers by CO_2. J Appl Polym Sci. 1985;30(6):2633–42.
(12) Oosawa F, Asakura S. Surface tension of high-polymer solutions. J Chem Phys. 1954;22(7):1255.
(13) Lee M, Park CB, Tzoganakis C. Measurements and modeling of PS/supercritical CO_2 solution viscosities. Polym Eng Ence. 2010;39(1):99–109.
(14) Hatano A. Dynamics of polyelectrolyte solutions. II. The polymer viscosity. J Phys Soc Jpn. 1981;50(1):295–314.
(15) Signorini GF, Jean-Louis Barrat, Klein ML. Structural relaxation and dynamical correlations in a molten state near the liquid-glass transition: A molecular dynamics study. J Chem Phys. 1990;92(2):1294–303.
(16) Righetti MC, Ajroldi G, Pezzin G. The glass transition temperature of polymer-diluent systems. Polymer. 1992;33(22):4779–85.
(17) Sato Y, Fujiwara K, Takikawa T, Sumarno, Takishima S, Masuoka H. Solubilities and diffusion coefficients of carbon dioxide and nitrogen in polypropylene, high-density polyethylene, and polystyrene under high pressures and temperatures. Fluid Phase Equilibria. 1999;162(1):261–76.
(18) Sato Y, Takikawa T. Solubility and diffusion coefficient of carbon dioxide in biodegradable polymers. Ind Eng Chem. 2000;39:4813–9.
(19) Sato Y, Takikawa T, Takishima S, Masuoka H. Solubilities and diffusion coefficients of carbon dioxide in poly(vinyl acetate) and polystyrene. J Supercrit Fluids. 2001;19(2):187–98.
(20) Sato Y, Takikawa T, Yamane M, Takishima S, Masuoka H. Solubility of carbon dioxide in PPO and PPO/PS blends. Fluid Phase Equilibria. 2002;194(5):847–58.
(21) Aionicesei E, Škerget M, Knez Ž. Measurement of CO_2 solubility and diffusivity in poly(L-lactide) and poly(L-lactide-co-glycolide) by magnetic suspension balance. J Supercrit Fluids The. 2008;47(2):296–301.
(22) Aionicesei E, Škerget M, Knez Ž. Measurement and modeling of the CO_2 solubility in poly(ethylene glycol) of different molecular weights. J Chem Eng Data. 2007;53(1):185–8.
(23) Yang Y, Narayanan Nair AK, Sun S. Adsorption and diffusion of methane and carbon dioxide in amorphous regions of cross-linked polyethylene: A molecular simulation study. Ind Eng Chem Res. 2019;124(7):1301–10.
(24) Yang Y, Narayanan Nair AK, Sun S. Adsorption and diffusion of methane and carbon dioxide in amorphous regions of cross-linked polyethylene: A molecular simulation study. Ind Eng Chem Res. 2019;58(19):8426–36.
(25) Yoshinori K, Keishin M, Yasutoshi N, Takuji H. Gas sorption in poly(vinyl benzoate). J Polym Sci Part B Polym Phys. 1986;24:535.
(26) Wong B, Zhang Z, Handa YP. High-precision gravimetric technique for determining the solubility and diffusivity of gases in polymers. J Polym Sci Part B Polym Phys. 1998;36:2025.
(27) Kamiya Y, Mizoguchi K, Terada K, Fujiwara Y, Wang JS. CO_2 sorption and dilation of poly(methyl methacrylate). Macromolecules. 1998;31(2):472–8.
(28) Lee JG, Flumerfelt RW. Nitrogen solubilities in low-density polyethylene at high temperatures and high pressures. 1995;58(12):2213–9.

(29) Eslami H, Kesik M, Karimi-Varzaneh HA, Müller-Plathe F. Sorption and diffusion of carbon dioxide and nitrogen in poly(methyl methacrylate). J Chem Phys. 2013;139(12):124902.
(30) Upreti SR, Mehrotra AK. Experimental measurement of gas diffusivity in bitumen: Results for carbon dioxide. Ind Eng Chem Res. 2000;39(4):1080–7.
(31) Rasmussen ML, Civan F. Parameters of gas dissolution in liquids obtained by isothermal pressure decay. Aiche J. 2010;55(1):9–23.
(32) Sheikha H, Mehrotra AK, Pooladi-Darvish M. An inverse solution methodology for estimating the diffusion coefficient of gases in Athabasca bitumen from pressure-decay data. J Pet Sci Eng. 2006;53(3–4):189–202.
(33) Sheikha H, Pooladi-Darvish M, Mehrotra AK. Development of graphical methods for estimating the diffusivity coefficient of gases in bitumen from pressure-decay data. Energy Fuels. 2005;19(5):2041–9.
(34) Chang F. A new fitting equation for supercritical CO_2 compression factor experimental data. J Guizhou Univ Technol. 2005;34(6):0193–7.
(35) Park GS. The mathematics of diffusion: J. Crank Clarendon Press, Oxford, 1975. 2nd edn. 414 pp. 12.50. Polymer. 1975;16(11):855.